

# The transport of water in a tetrafunctional epoxy resin by near-infrared Fourier transform spectroscopy

P. Musto<sup>a,\*</sup>, L. Mascia<sup>b</sup>, G. Ragosta<sup>a</sup>, G. Scarinzi<sup>a</sup>, P. Villano<sup>a</sup>

<sup>a</sup>*Institute of Research and Technology of Plastic Materials, National Research Council of Italy, Via Toiano, 6, 80072, Arco Felice, Naples, Italy*

<sup>b</sup>*Institute of Polymer Technology and Materials Engineering, Loughborough University, Loughborough LE11 3TU, UK*

Received 20 October 1998; received in revised form 15 February 1999; accepted 12 March 1999

---

## Abstract

An epoxy resin formulation composed of tetraglycidyl-4,4'-diamino diphenylmethane (TGDDM) and 4,4'-diamino diphenyl sulfone (DDS) was investigated by Fourier transform near infrared (FT-NIR) spectroscopy and dynamic-mechanical analysis. Both techniques have demonstrated the essentially complete cure state of the resin with the adopted curing schedule. A novel feature of this work is the possibility of monitoring the transport of water into the resin by using of an FT-NIR spectrometer as a detector in place of the currently employed gravimetric detectors. The data gathered at different temperatures have revealed a good agreement with conventional gravimetric measurements, which verifies the reliability and accuracy of the experimental approach presented herein. © 1999 Elsevier Science Ltd. All rights reserved.

*Keywords:* FT-NIR spectroscopy; Epoxy resins; Diffusion

---

## 1. Introduction

The tetrafunctional epoxy resin tetraglycidyl-4,4'-diamino diphenylmethane (TGDDM) cured with the aromatic diamine 4,4'-diamino diphenyl sulfone (DDS), is one of the most widely employed matrices for the production of high performance fibre composites in the aircraft and spacecraft industries [1,2]. The attractive features of this thermosetting resin are its low density combined with high tensile strength and modulus, and a very high  $T_g$  combined with good thermal and chemical resistance [3,4].

It has, however, a very serious drawback for these applications, related to the absorption of large amounts of water, which brings about a deterioration in mechanical properties in hot moist environments. At equilibrium, a typical TGDDM/DDS cured system may absorb between 4.0 and 6.5 wt.% of water [5–7], depending on the stoichiometry of the formulation and on curing conditions. The absorbed water acts as a very efficient plasticizer, strongly reducing the  $T_g$  of the resin, typically by 20°C for every 1% of absorbed water [4,6,7].

Furthermore, if water absorption takes place at elevated

temperatures and/or for prolonged time periods, a permanent damage of the structural network may ensue, which can give rise to the formation of microcracks and result into catastrophic failures [2–4,7].

The mechanism of moisture absorption in the various types of epoxy has been widely investigated, but it is still not fully understood. One important issue is the state of aggregation of the water molecules within the bulk of the material. The penetrant population can be divided into molecules forming an ordinary polymer–diluent solution and those absorbed onto hydrophilic sites or trapped into the “excess” free volume frozen in the glass structure. Due to the multiplicity of states of the penetrant molecules within the matrix, the overall penetrant up-take cannot be considered as a reliable measure of the degree of plasticization.

Another relevant and controversial issue concerns the kind of molecular interactions between the water molecules and the epoxy network. Several spectroscopic studies, notably by solid-state NMR spectroscopy [8,9], have addressed this point. Fourier transform infrared (FTIR) spectroscopy in the mid infrared range has also been employed [10,11], but no definitive conclusions have been reached so far. This approach is exploited further in the present work.

Thus an experimental set-up has been developed, based on FTIR spectroscopy measurements, to monitor in situ and

---

\* Corresponding author.

E-mail address: musto@mail.irtemp.na.cnr.it (P. Musto)

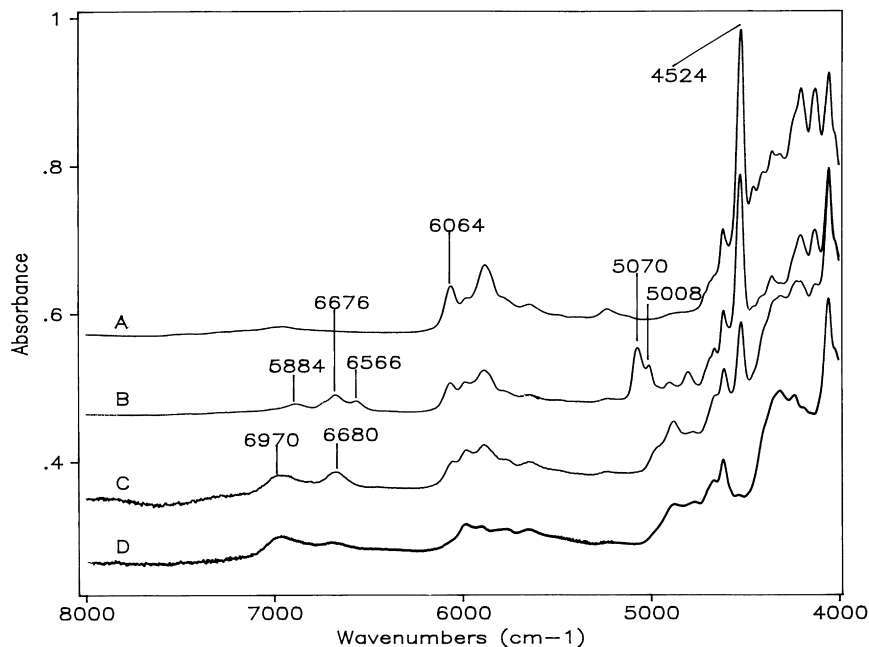


Fig. 1. FT-NIR transmission spectra in the wave-number range 8000–4000  $\text{cm}^{-1}$ . Trace A: uncured TGDDM; trace B: uncured TGDDM/DDS resin; trace C: TGDDM/DDS resin after curing at 140°C for 16 h; trace D: TGDDM/DDS resin after post-curing at 200°C for 4 h.

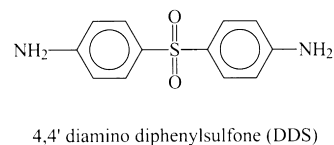
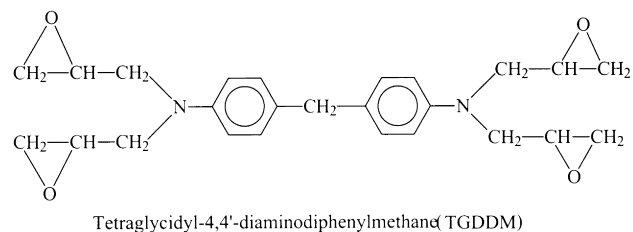
in real-time the transport process of water within a TGDDM resin cured with DDS. A near-infrared (NIR) wavenumber range between 8000–4000  $\text{cm}^{-1}$  was chosen instead of the more widely employed mid infrared range (MIR, 4000–400  $\text{cm}^{-1}$ ) for two reasons. The first is the intense and characteristic spectrum of water in the NIR range. The second reason is related to the fact that in the NIR interval are located the overtone and combination bands, whose intensity is about one order of magnitude lower than that of the corresponding fundamentals occurring in the MIR range. This makes it possible to use thick samples, i.e. up to several millimetres, without losing the absorbance linearity with concentration of their spectra. Conversely, in the MIR interval the sample thickness cannot exceed 50  $\mu\text{m}$  in order to remain within the absorbance range in which the Beer–Lambert law is valid. For such thin specimens the mass transport is very rapid and it would be difficult to study the relevant events even with a fast-scanning technique, such as FTIR spectroscopy.

## 2. Experimental

### 2.1. Materials and curing schedule

The epoxy resin was a commercial grade of tetraglycidyl-4,4'-diamino diphenylmethane (TGDDM) supplied by Ciba Geigy (Basel, Switzerland) and the curing agent was 4,4'-diamino diphenylsulphone (DDS) from Aldrich

(Milwaukee, WI, USA). The chemical formulae of both components is shown below:



The resin mixture was prepared by dissolving 30 g of DDS in 100 g of TGDDM at 130°C with vigorous mechanical stirring. After complete dissolution, the mixture was degassed under vacuum at the same temperature and immediately poured in a stainless steel mould. Curing was conducted at 140°C for 16 h and was followed by a post-curing step at 200°C for 4 h.

### 2.2. Characterization techniques

FT-NIR spectra were recorded in the transmission mode

on samples 0.10–0.25 mm thick using a Perkin–Elmer System 2000 spectrometer. This instrument was equipped with a high temperature tungsten halogen NIR source, a multi-layer calcium fluoride beam-splitter and a deuterated triglycine sulphate (DTGS) detector. The scanned wavenumber range was 8000–4000  $\text{cm}^{-1}$ ; 10–300 scans were co-added for each measurement to improve the signal-to-noise ratio. The isothermal desorption measurements were carried out in an environmental chamber constructed in house by modifying the commercially available SPECAC 20100 cell. The chamber was directly mounted in the spectrometer to monitor the process in real-time. This allowed, at the same time, careful control of the main process parameters, such as temperature, pressure and environment. The measurements were carried out at 22, 35, 45 and 60°C with an accuracy of  $\pm 0.5^\circ\text{C}$ , under a  $\text{N}_2$  atmosphere and a pressure of 760 Torr.

Gravimetric sorption measurements were carried out by the so called pat-and-weight technique. Samples (0.10–0.25 mm thick) were dried overnight at 100°C under vacuum to ensure complete removal of absorbed water, which was confirmed by FT-NIR spectroscopy. The dried specimen was immersed in a deionized water bath thermostatically controlled at  $22(\pm 0.1)^\circ\text{C}$ . Periodically, the sample was removed, blotted and weighed with an analytical laboratory balance. The associated FT-NIR spectrum was also recorded in order to correlate the gravimetric results with the spectroscopic data.

Dynamic-mechanical measurements were made on the same samples used for spectroscopic and sorption measurements, in the dry state. A Polymer Laboratories DMTA MKIII apparatus was used, at 1 Hz in the single-cantilever bending mode.

### 3. Results and discussion

#### 3.1. Characterization of the cured resin

In Fig. 1 are reported the transmission FTIR spectra (NIR wavenumber range, 8000–4000  $\text{cm}^{-1}$ ) for the uncured TGDDM resin (trace A), the uncured TGDDM/DDS formulation (trace B) and the same mixture after curing and post-curing (traces C and D, respectively).

Two characteristic peaks attributed to the oxirane ring can be identified in traces A and B at 6064  $\text{cm}^{-1}$  and at 4524  $\text{cm}^{-1}$  [12–18]. The peak at higher frequency is due to the first overtone of the terminal  $\text{CH}_2$  stretching mode, while the peak at lower frequency has been attributed to a combination band of the second overtone of the epoxy ring stretch at 916  $\text{cm}^{-1}$  with the fundamental C–H stretch at about 2725  $\text{cm}^{-1}$  [18]. The intensity of both absorptions is reduced considerably after curing and disappear almost completely after post-curing. A further interesting wavenumber region is the one between 5100 and 5000  $\text{cm}^{-1}$ . Here a partially resolved doublet is found in the presence

of the diamine hardener (see trace B), with maxima at 5070 and 5008  $\text{cm}^{-1}$ . These peaks are characteristic of the primary amine groups: the 5070  $\text{cm}^{-1}$  peak is assigned to a combination of the  $\nu_{\text{s,N-H}}$  fundamental at 3464  $\text{cm}^{-1}$  and the  $\delta_{\text{N-H}}$  deformation at 1630  $\text{cm}^{-1}$ , while the 5008  $\text{cm}^{-1}$  peak is due the combination of the  $\nu_{\text{as,N-H}}$  mode at 3367  $\text{cm}^{-1}$  and the same  $\delta_{\text{N-H}}$  deformation. This doublet completely disappears in trace C, indicating that the primary amino groups are already reacted to full conversion even after the low temperature curing step.

The wavenumber region between 7500 and 6200  $\text{cm}^{-1}$  is rather complex for the uncured TGDDM/DDS mixture (trace B), owing to the simultaneous presence of the overtones of the O–H and N–H stretching modes. The hydroxyl groups in the uncured TGDDM are due to partial hydrolysis of the oxirane rings, which accounts for the 14.0% (by mole) reduction of the above groups with respect to the stoichiometric content, as determined by potentiometric titration. In particular, the first overtone of the  $\nu_{\text{O-H}}$  is located at 6884  $\text{cm}^{-1}$  while the overtones of the  $\nu_{\text{s,N-H}}$  and the  $\nu_{\text{as,N-H}}$  occur at 6676 and at 6566  $\text{cm}^{-1}$ , respectively.

After curing, the complex profile in this frequency range changes substantially: a broad absorption is observed at 6970  $\text{cm}^{-1}$ , with a minor component superimposed along the low frequency side, and centred at 6680  $\text{cm}^{-1}$ . The peak at 6970  $\text{cm}^{-1}$  is due to hydroxyl groups and the increase in intensity with respect to the spectrum of the uncured resin reflects the increase in concentration of the O–H groups during curing. The upward shift with respect to the peak position prior to curing reflects the formation of a more complex and extended hydrogen-bonding network among the OH groups.

The 6680  $\text{cm}^{-1}$  peak is due to the first overtone of the  $\nu_{\text{N-H}}$  fundamental of the secondary amine groups located at 3385  $\text{cm}^{-1}$ . As shown by spectrum C of Fig. 1, a considerable amount of secondary amine groups remain unreacted after curing. Post-curing brings about a further increase in the hydroxyl group concentration and a reduction in concentration of secondary amine groups.

From the spectra of Fig. 1 it is possible to estimate quantitatively the conversion,  $\alpha$ , of reactive species present in the system, relative to their initial concentration, i.e.

$$\alpha = \left( \frac{C_0 - C_f}{C_0} \right) \times 100 = \left( 1 - \frac{C_f}{C_0} \right) \times 100$$

where  $C_0$  and  $C_f$  are the concentration of the reactive groups before and after the reaction, respectively, hence from the Beer–Lambert law

$$\alpha = \left( 1 - \frac{\bar{A}_f}{\bar{A}_0} \right) \times 100$$

where  $\bar{A}_f$  represents the absorbance of the analytical peak after the reaction, normalized for the sample thickness (reduced absorbance), and  $\bar{A}_0$  is the same parameter recorded on the specimen prior to curing. The determination of the secondary amine conversion from the 6680  $\text{cm}^{-1}$

Table 1  
Conversion of the reactive groups in the TGDDM/DDS formulation after the curing and post-curing processes, as evaluated by FT-NIR spectroscopy

Group	Peak (cm <sup>-1</sup> )	$\alpha_c^a$ (%)	$\alpha_{pc}^b$ (%)
Epoxy	6065	59	97
Primary amine	5071	100	100
Secondary amine	6675	54	84

<sup>a</sup> Conversion after curing (16 h, 140°C).

<sup>b</sup> Conversion after post-curing (4 h, 200°C).

peak, which is initially superimposed onto the primary amine doublet, was performed according to the method described elsewhere [19].

The values of  $\alpha$  for the different reactive groups after curing and post-curing, are collectively reported in Table 1. The data reported therein indicate the essentially complete cure of the formulation, and this conclusion is confirmed by the absence of any residual heat of reaction in the DSC thermogram of the specimen.

In Fig. 2 is reported the dynamic-mechanical spectrum expressed in term of  $\tan\delta$  and storage modulus,  $E'$ , of the sample after the curing and post-curing protocols. The curves of  $\tan\delta$  and  $E'$  as a function of temperature and the  $T_g$  value obtained therefrom (270°C) are characteristic of a fully cured TGDDM/DDS resin [1–4].

### 3.2. Gravimetric and spectroscopic diffusion measurements

Sorption data at 22°C, measured gravimetrically on a film sample of TGDDM/DDS cured resin 0.220 mm thick, are reported in Fig. 3 as Fickian diffusion plots, that is as  $M_t/M_\infty$  vs (time)<sup>0.5</sup> L<sup>-1</sup>. As usual,  $M_t$  and  $M_\infty$  represent the mass of penetrant absorbed at time  $t$  and at equilibrium, respectively, and  $L$  is the sample thickness. The absorption isotherm displays a pronounced linear region extending up to about 80% of the total absorption range.

For a plane polymer sheet exposed to a diffusing fluid, the change of the concentration of the diffusant,  $C$ , at distance  $x$  from the contacting surface as a function of time,  $t$ , is expressed by Fick's second law [20–23]:

$$\frac{\partial C}{\partial t} = D \frac{\partial^2 C}{\partial x^2} \quad (1)$$

where  $D$  represents the diffusion coefficient. If the initial concentration,  $C_0$ , of the diffusant is constant at the surface and reaches a value  $C_{\max}$  at equilibrium, then the solution of Eq. (1) gives [20–23]:

$$\frac{C - C_0}{C_{\max} - C_0} = 1 - \frac{4}{\pi} \sum_{n=0}^{\infty} \frac{(-1)^n}{2n+1} \exp\left[\frac{-D(2n+1)^2\pi^2 t}{L^2}\right] \cos\left[\frac{(2n+1)\pi x}{L}\right] \quad (2)$$

where  $n$  is an integer. The mass  $M$ , of diffusant taken up by the polymer as a function of time, is obtained by integrating Eq. (2) over the entire thickness,  $L$  i.e.

$$\frac{M_t}{M_\infty} = 1 - \frac{8}{\pi^2} \sum_{n=0}^{\infty} \frac{1}{(2n+1)^2} \exp\left[\frac{-D(2n+1)^2\pi^2 t}{L^2}\right] \quad (3)$$

For  $M_t/M_\infty$  ratios less than 0.6, Eq. (3) may be approximated by the expression:

$$\frac{M_t}{M_\infty} = \frac{4}{L} \left(\frac{Dt}{\pi}\right)^{1/2} \quad (4)$$

which provides a simple method for the determination of the diffusion coefficient,  $D$ , by measuring the initial slope of the plot  $M_t/M_\infty$  vs (time)<sup>0.5</sup> L<sup>-1</sup>. The value of  $D$ , obtained in this way, from the curve in Fig. 3, is equal to  $1.10 \times 10^{-9}$  cm<sup>2</sup> s<sup>-1</sup>.

Fig. 4 shows the FT-NIR spectra in the wavenumber range 8000–4000 cm<sup>-1</sup> for the dry epoxy resin (trace A)

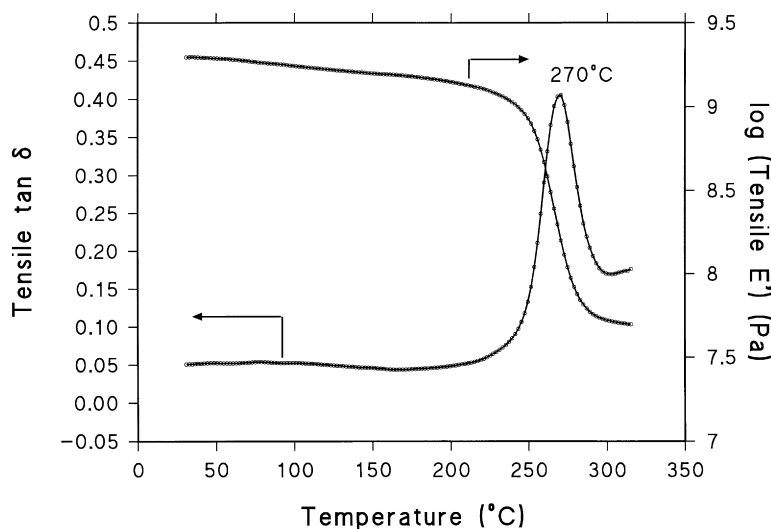


Fig. 2. Dynamic-mechanical spectra expressed in terms of  $\tan\delta$  and storage modulus ( $E'$ ) in the temperature range 25–330°C of the cured TGDDM/DDS resin.

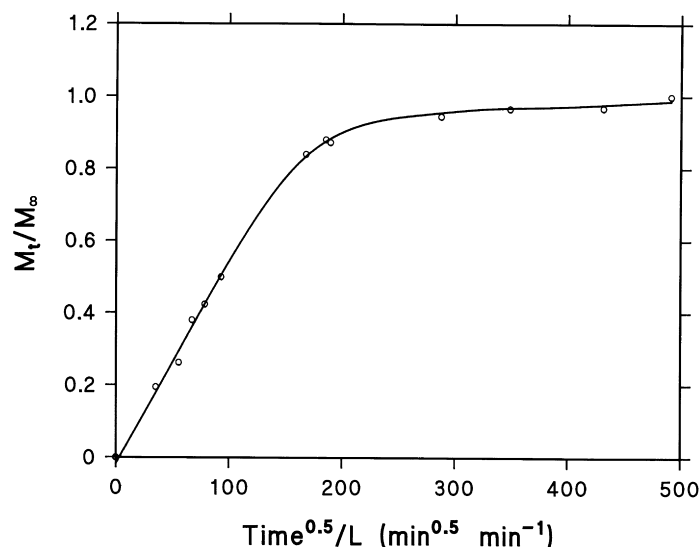


Fig. 3. Fick's plot relative to isothermal sorption of water into the TGDDM/DDS resin at 22°C.

and for the same resin having absorbed the equilibrium amount of water (6.5 wt.%, trace B).

A characteristic peak attributed to the presence of water is immediately apparent at  $5210\text{ cm}^{-1}$  and is assigned to a combination of the  $\nu_{\text{as}}$  and  $\delta$  fundamentals which occur, respectively, at  $3755$  and at  $1595\text{ cm}^{-1}$  in the vapour phase spectrum of water. The peak at  $5210\text{ cm}^{-1}$  is well resolved, free from interference by the polymeric substrate spectrum, and of sufficient intensity to be considered a suitable candidate for the spectroscopic determination of the water content in the sample.

A further water sensitive absorption, due to the combination of the  $\nu_{\text{as}}$  and  $\nu_{\text{s}}$  fundamentals, is located around

$6900\text{ cm}^{-1}$ . This component is superimposed on the much stronger  $\nu_{\text{OH}}$  overtone due to the hydroxyl groups of the epoxy resin, which prevents its detection. A method based on spectral subtraction analysis has been developed, however, to isolate the water spectrum in this frequency range. This spectrum provides important information at molecular level regarding the interaction between the penetrant molecules and the polymeric substrate, as well as an insight into the state of aggregation of the penetrant molecules. This information will be discussed in detail in the second part of this series of articles [24].

In Fig. 5 is reported the integrated absorbance of the water sensitive peak at  $5210\text{ cm}^{-1}$ , normalized for the

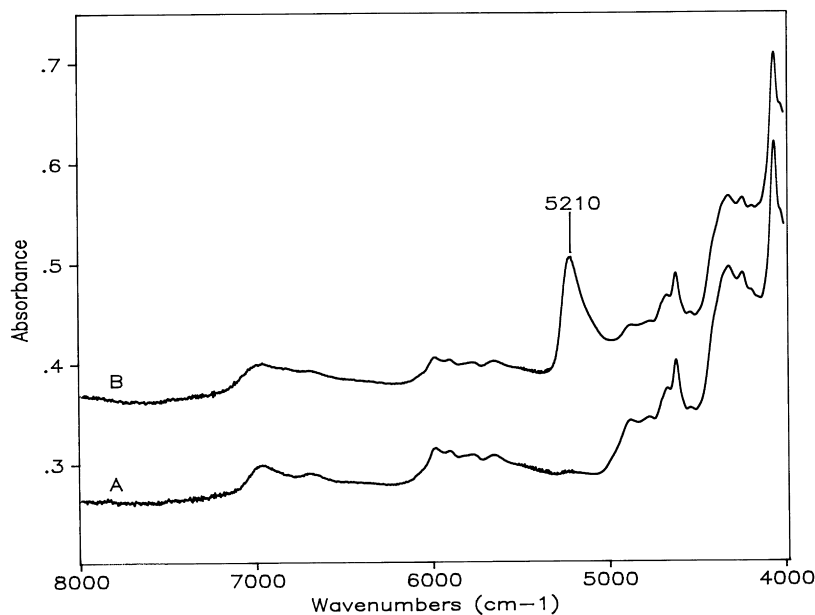


Fig. 4. FT-NIR transmission spectra in the wavenumber range  $8000\text{--}4000\text{ cm}^{-1}$  relative to the dry TGDDM/DDS resin (trace A) and to the same resin after water saturation (trace B).

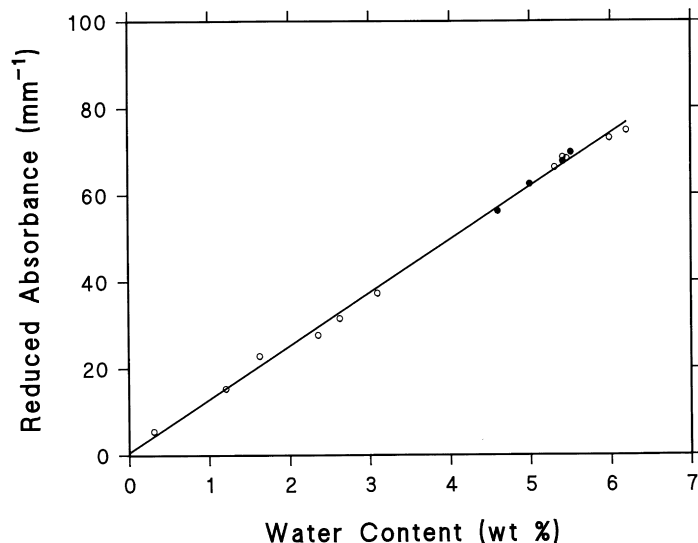


Fig. 5. Calibration curve of the integrated absorbance normalized for sample thickness (reduced absorbance) of the  $5210\text{ cm}^{-1}$  peak vs. water content for the TGDDM/DDS resin. The open symbols refer to specimens 0.220 mm thick. The solid symbols are for specimens 2.75 mm thick.

sample thickness, as a function of the water content in the sample, determined gravimetrically. This plot gives a straight line passing through the origin, with a correlation coefficient,  $r^2$ , equal to 0.997 and a slope of 12.18 absorbance units  $(\text{wt.}\% \text{ of water})^{-1}$ . This diagram demonstrates that the analytical peak behaves according to the Beer–Lambert law over the whole concentration range of water in the resin, and makes it possible direct and precise evaluation of the water content by spectroscopic means. The same calibration curve can be employed also for much thicker samples, as demonstrated by the solid symbols, which were obtained for specimens 2.75 mm thick.

To study in more detail the transport of water through the TGDDM/DDS resin by FT-NIR spectroscopy, the isothermal desorption mode was used, in order to eliminate the spectroscopic interference from liquid water. In a transmission measurement, in fact, this would prevent the detection of water absorbed in the polymeric substrate.

In Fig. 6 are shown the FT-NIR transmission spectra in the wavenumber range  $6100\text{--}4500\text{ cm}^{-1}$ , collected at various time intervals during the desorption experiment at  $22^\circ\text{C}$ . These reveal the gradual decrease of the  $5210\text{ cm}^{-1}$  peak, due to the depletion of the penetrant molecules from the polymer matrix. The integrated absorbance of the above

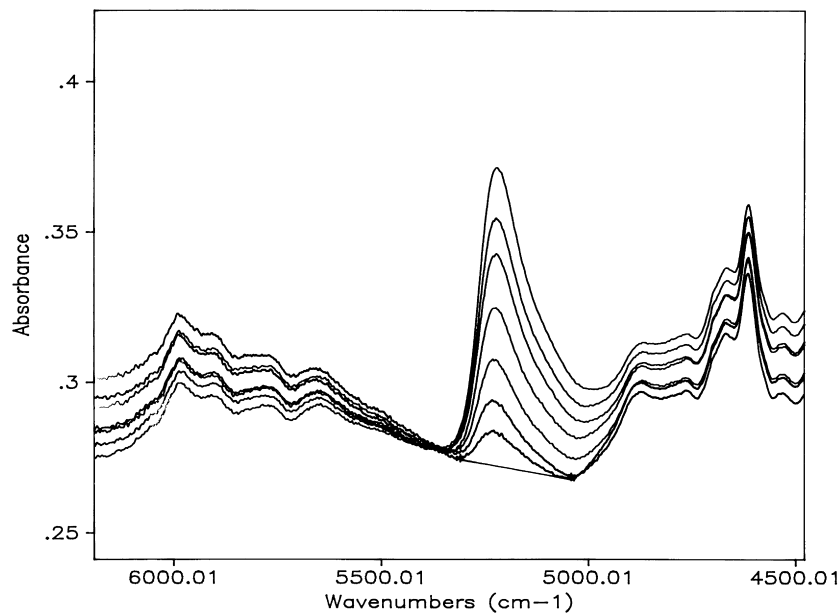


Fig. 6. FT-NIR transmission spectra collected at different times in the frequency range  $6100\text{--}4500\text{ cm}^{-1}$  during the desorption measurement carried out at  $22^\circ\text{C}$ . The baseline for the evaluation of the peak area is also indicated.

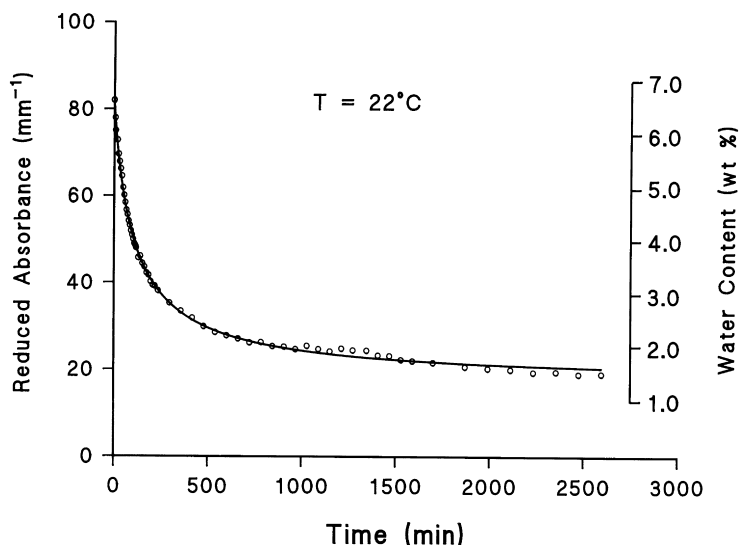


Fig. 7. Reduced absorbance of the 5210 cm<sup>-1</sup> peak as a function of time for the desorption measurement carried out at 22°C. The right Y-axis indicates the per cent water content of the specimen.

peak, corrected for the sample thickness (reduced absorbance) is plotted, as a function of time, in Fig. 7, showing also the concentration data obtained with the use of the calibration curve in Fig. 5. Such information is provided by the second ordinate scale of Fig. 7.

The absorbance data make it possible to calculate the absolute parameters of the diffusion process [21,22]. Due to the invariance of the film thickness during the measurements, we may write:

$$\frac{A_0 - A_t}{A_0 - A_\infty} = \frac{C_0 - C_t}{C_0 - C_\infty} = \frac{M_t}{M_\infty} \quad (5)$$

Here  $C_0$ ,  $C_t$  and  $C_\infty$  represent, respectively, the concentration of water into the sample at times 0,  $t$  and at equilibrium.

Therefore  $C_0 - C_t = M_t$  and  $C_0 - C_\infty = M_\infty$  represent the mass of water desorbed from the sample at time  $t$  and at equilibrium, respectively. The Fick's plot obtained from the spectral data of Fig. 7 is shown in Fig. 8, together with the curve for the gravimetric absorption measurement, for comparison. The difference between the two curves is minimal and may safely be considered to be within experimental error. This result confirms the reliability of the spectroscopic approach to follow the diffusion of water through films and indicates that, for the system under investigation, the absorption and the desorption processes are equivalent. This is not surprising when considering that the dry polymer has a  $T_g$  of 270°C, which reduces to 180°C [25] after water saturation. Thus at 22°C the material is well below its  $T_g$ ,

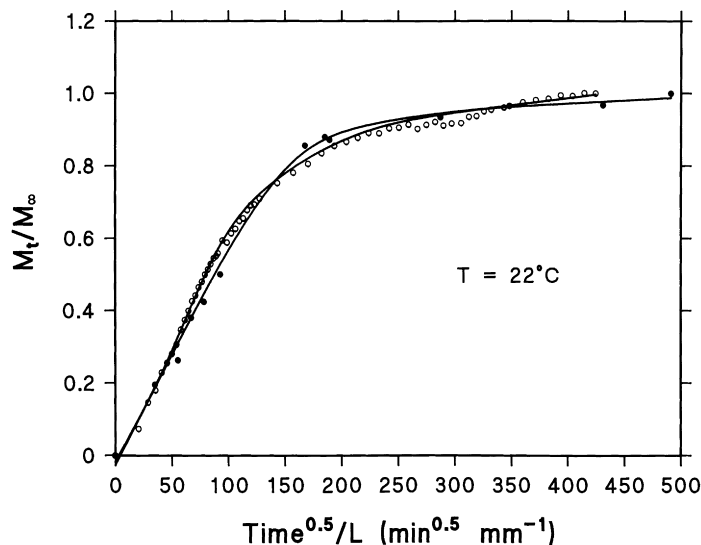


Fig. 8. Comparison between the sorption curve obtained gravimetrically (●) and the desorption curve obtained by FT-NIR spectroscopy (○) for the TGDDM/DDS resin at 22°C.

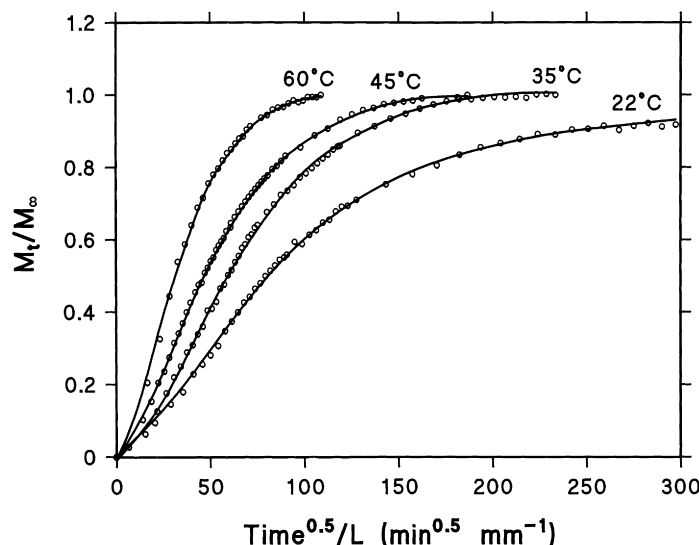


Fig. 9. Desorption curves obtained via FT-NIR spectroscopy at the various temperatures.

and this rigid glass phase is not altered by the presence of the penetrant molecules.

The diffusion coefficient for desorption, calculated from the data in Fig. 8, is  $1.52 \times 10^{-9} \text{ cm}^2 \text{ s}^{-1}$ , which is very close to the value obtained from the gravimetric sorption experiment.

The desorption curves at 22, 35, 45 and 60°C are collectively reported in the form of Fick's diagrams, in Fig. 9. The overall shape is similar, apart from the initial slope which obviously increases with increasing temperature; this is indicative of the invariance of the diffusion mechanism over the temperature range investigated. A linear region is displayed in all curves, extending up to ordinate values of about 0.8 and provides a reliable method for the determination of the diffusion coefficients; these are collectively reported in Table 2.

The temperature dependence of the diffusion coefficients can be expressed by an Arrhenius-type relationship [21–23]:

$$D = D_0 \exp\left(-\frac{E_a}{RT}\right) \quad (6)$$

where the pre-exponential factor  $D_0$  represents the

Table 2  
Diffusion coefficients for the TGDDM/DDS resin at the various investigated temperatures

Temperature (°C)	Temperature (K)	Diffusion coefficient ( $\text{cm}^2 \text{ s}^{-1}$ ) $\times 10^9$
22	295	1.53
36	309	3.05
45	318	4.49
60	333	9.97

permeability index [6,26],  $E_a$  is the activation energy of the diffusion process and  $R$  is the gas constant.

The plot of  $\ln D$  vs.  $1/T$  in Fig. 10, is linear, with a correlation coefficient,  $r^2$ , of 0.995. The values of  $E_a$  and  $D_0$ , calculated from the slope and intercept of the above straight line are  $9.5 \text{ kcal mol}^{-1}$  and  $1.8 \times 10^{-2} \text{ cm}^2 \text{ s}^{-1}$ , respectively. The coincidence of sorption and desorption curves allows a comparison of the results obtained in the present investigation with those reported in the literature for analogous systems obtained by gravimetric sorption measurements at different temperatures. For instance the above  $E_a$  and  $D_0$  values compare quite favourably with those reported by Diamant et al. [26], who investigated the effect of modifying the network structure on moisture absorption in the case of a difunctional epoxy resin (Epon 828) cured with aromatic diamine hardeners. In fact these systems yielded diffusion coefficients varying from  $0.83 \times 10^{-9} \text{ cm}^2 \text{ s}^{-1}$  at 25°C to  $10.2 \times 10^{-9} \text{ cm}^2 \text{ s}^{-1}$  at 70°C. The values of  $E_a$  were very close, i.e. from 11.6 to 11.8  $\text{kcal mol}^{-1}$  and  $D_0$  ranged from 0.24 to 0.30  $\text{cm}^2 \text{ s}^{-1}$ .

The diffusion of water in a tetrafunctional epoxy/aromatic diamine formulation (Narmco 5208) was investigated as a function of temperature by McKague and colleagues [6]. They reported an activation energy for the diffusion of water equal to 8.06  $\text{kcal mol}^{-1}$ , which is in close agreement with the value obtained in this work. The  $D_0$  value of  $5.14 \times 10^{-4} \text{ cm}^2 \text{ s}^{-1}$ , however, is 35 times lower than the value obtained in the present contribution. Such a discrepancy is to be ascribed partly to the inherent inaccuracy in the calculation of  $D_0$ , which involves extrapolation over a wide abscissa range, and also to differences in the molecular structure and/or the stoichiometry of the reactants in the two formulations in question.

For Fiberite 934, which is an epoxy formulation containing 63.2 wt.% TGDDM, 25.3 wt.% DDS, 11.2 wt.% bisphenol-A epoxy resin and 0.3 wt.%  $\text{BF}_3$  catalyst complex,



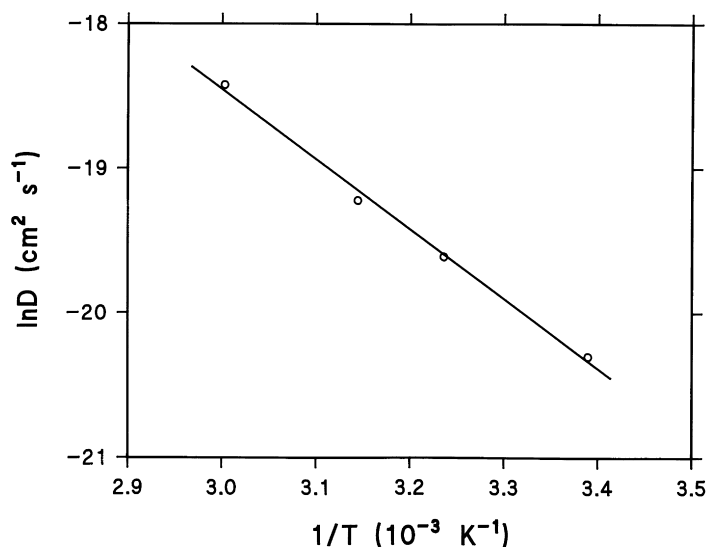


Fig. 10. Arrhenius plot of the diffusion coefficients.

Majerus and co-workers reported [5] an activation energy of  $8.8 \text{ kcal mol}^{-1}$  and a  $D_0$  value of  $1.56 \times 10^{-3} \text{ cm}^2 \text{ s}^{-1}$ . These results compare even more favourably with those reported in the present work.

The agreement between the absolute parameters of diffusion obtained in the present work with those reported in the literature confirms, on one hand, the reliability and accuracy of the spectroscopic approach to monitor the diffusion process. On the other hand this comparison indicates that the type of resin (bifunctional, tetrafunctional or a mixture of the two) has a limited influence on these parameters. It is reasonable to conclude that the dominant factor is represented by the functionality and molecular structure of the hardener, which is the same (DDS) for all the cases compared above.

#### 4. Conclusions

A tetrafunctional epoxy resin, cured by an aromatic diamine hardener has been characterized with respect to the degree of cure by Fourier transform near infrared (FT-NIR) spectroscopy and dynamic-mechanical analysis. Both techniques indicated the essentially complete cure of the formulation in the conditions employed. The transport properties of the above resin have been investigated at different temperatures by a novel experimental approach which makes use of FT-NIR spectroscopy for detecting in situ the concentration of water into the sample. The feasibility and accuracy of this approach is demonstrated in comparison with conventional gravimetric measurements. An activation energy for desorption of  $9.5 \text{ kcal mol}^{-1}$  and a  $D_0$  value of  $1.8 \times 10^{-2} \text{ cm}^2 \text{ s}^{-1}$  were calculated, which are in good agreement with literature results obtained by gravimetric measurements, particularly in the case of the activation energy value. This comparison indicate that the main

factor affecting the diffusion parameters is not the type of epoxy resin (bifunctional, tetrafunctional or a mixture of the two) but rather the functionality and molecular structure of the hardener.

#### Acknowledgements

Thanks are due to Mr. V. Di Liello for helping in the design and construction of the environmental chamber for FTIR desorption measurements and to Mr. A. Lahoz for technical assistance in the spectroscopic measurements. One of us (P.M.) acknowledges financial support by the National Research Council of Italy (CNR) "Short Term Mobility Program" 1996-1997, for his stay at Loughborough University to consolidate aspects of this work.

#### References

- [1] Lee H, Neville K. Handbook of epoxy resins. New York: McGraw-Hill, 1990.
- [2] Gillham JK. Encyclopaedia of polymer science and technology. 2. New York: Wiley, 1986 pp. 519–24.
- [3] May CA, editor. Epoxy resins, chemistry and technology 2. New York: Marcel Dekker, 1988.
- [4] Ellis B, editor. Chemistry and technology of epoxy resins Glasgow: Blackie Academic and Professional, 1993.
- [5] Majerus MS, Soong DS, Prausnitz JM. J Appl Polym Sci 1984;29:2453.
- [6] McKague EL, Reynolds JD, Halkies JE. J Appl Polym Sci 1978;22:1643.
- [7] Mijovic J, Lin K. J Appl Polym Sci 1985;30:2527.
- [8] Jelinski LW, Dumais JJ, Chiolli AL, Ellis TS, Karasz FE. Macromolecules 1985;18:1091.
- [9] Banks L, Ellis B. Polym Bull 1979;1:377.
- [10] Levy RL, Fanter DL, Summers CJ. J Appl Polym Sci 1979;24:1643.
- [11] Antoon MK, Koenig JL, Serafini T. J Polym Sci: Polym Phys Ed 1981;19:1567.
- [12] Whetsel KB. Appl Spectrosc Rev 1968;2:1.

- [13] Weyer LG. *Appl Spectrosc Rev* 1985;21:1.
- [14] Mijovic J, Andjelic S, Kenny JM. *Polym Adv Technol* 1996;7:1.
- [15] Xu L, Schlup JR. *Appl Spectrosc* 1996;50:109.
- [16] George GA, Cole-Clarke P, St. Johon N, Friend G. *J Appl Polym Sci* 1991;42:643.
- [17] Fu JH, Schlup JR. *J Appl Polym Sci* 1993;49:219.
- [18] Chike KE, Myrick ML, Lyon RE, Angel SM. *Appl Spectrosc* 1993;10:1631.
- [19] Musto P, Martuscelli E, Ragosta G, Russo P, Scarinzi G. Submitted to *J Appl Polym Sci*.
- [20] Crank J. *The mathematics of diffusion. 2*. Oxford: Oxford University Press, 1975.
- [21] Crank J, Park GS. *Diffusion in polymers*. New York: Academic Press, 1968.
- [22] Comyn J, editor. *Polymer permeability* London: Elsevier, 1985. pp. 20–27 Chapter 2.
- [23] Vieth WR. *Diffusion in and through polymers*. Munich: Hansen, 1991.
- [24] Musto P, Ragosta G, Mascia L. Submitted to *Macromolecules*.
- [25] Musto P, Martuscelli E, Ragosta G, Russo P, Scarinzi G. *J Appl Polym Sci* 1998;69:1029.
- [26] Diamant Y, Marom G, Broutman L. *J Appl Polym Sci* 1981;26:3015.